LETTER

doi:10.1038/nature13576

Hallucigenia's onychophoran-like claws and the case for Tactopoda

Martin R. Smith[1] & Javier Ortega-Hernández[1]

The Palaeozoic form-taxon Lobopodia encompasses a diverse range of soft-bodied 'legged worms' known from exceptional fossil deposits[1–9]. Although lobopodians occupy a deep phylogenetic position within Panarthropoda, a shortage of derived characters obscures their evolutionary relationships with extant phyla (Onychophora, Tardigrada and Euarthropoda)[2,3,5,10–15]. Here we describe a complex feature in the terminal claws of the mid-Cambrian lobopodian *Hallucigenia sparsa*—their construction from a stack of constituent elements—and demonstrate that equivalent elements make up the jaws and claws of extant Onychophora. A cladistic analysis, informed by developmental data on panarthropod head segmentation, indicates that the stacked sclerite components in these two taxa are homologous—resolving hallucigeniid lobopodians as stem-group onychophorans. The results indicate a sister-group relationship between Tardigrada and Euarthropoda, adding palaeontological support to the neurological[16,17] and musculoskeletal[18,19] evidence uniting these disparate clades. These findings elucidate the evolutionary transformations that gave rise to the panarthropod phyla, and expound the lobopodian-like morphology of the ancestral panarthropod.

Palaeozoic lobopodians feature prominently in discussions about the origins of crown-group panarthropods—the extant velvet worms (Onychophora), water bears (Tardigrada) and euarthropods (Euarthropoda)[5,9–11,20]. Although lobopodians have been regarded as onychophoran ancestors[2,3], the presence of 'primitive' characters—such as a terminal radial mouth, unsclerotized annulated cuticle, a non-segmented body and terminal claws in the walking legs—suggests a deeper phylogenetic position[1,4,13]. Because lobopodians have few derived morphological features in common with extant panarthropod phyla, there has been much disagreement over the precise affinities of these extinct organisms and their significance for the origins of the major extant groups[5,10–12,14,20,21].

Here we describe the fine morphology of exceptionally preserved terminal claws in the Burgess Shale lobopodian *H. sparsa* (mid-Cambrian; Stage 5), and demonstrate a fundamentally similar construction in the claws and jaws of the extant onychophoran *Euperipatoides kanangrensis*. These new data clarify both the affinity of ambiguous lobopodians and the evolutionary origins of extant panarthropods.

H. sparsa bears two types of sclerite: a pair of appendicular sclerites (claws) on each walking leg, and seven pairs of armature sclerites (spines) along the trunk (Fig. 1a). The claws form smooth curves that subtend an angle of 100°, and comprise a stack of three constituent elements (Fig. 1b–d), separated by 21° of displacement along a logarithmic curve denoted by the Raupian parameters[22] $W = 3$, $T = 0$, $D = 2$. The preserved carbon film thins gradually towards the base of the claw, reflecting a lesser degree of sclerotization.

Hallucigenia spines each comprise a stack of one to five constituent elements[6] that are separated by 1–6° along the logarithmic spiral given by $W = 3$, $T = 0$, $D = 1.07$. Spines that have been compressed obliquely to their plane of curvature express a smaller value of D, representing a preservational artefact (Extended Data Fig. 1). The surface of each constituent element is characterized by an ornament of regularly arranged scales (Extended Data Fig. 2).

Onychophorans lack armature sclerites, but possess two types of appendicular sclerite: paired terminal claws in the walking legs, and denticulate jaws within the mouth cavity[9,23]. As in *H. sparsa*, claws in *E. kanangrensis* exhibit a broad base that narrows to a smooth conical point (Fig. 1e–h). Each terminal claw subtends an angle of 130° and comprises two to three constituent elements (Fig. 1e–h). Each smaller element precisely fills the basal fossa of its container, from which it can be extracted with careful manipulation (Fig. 1e, g, h and Extended Data Fig. 3a–g). Each constituent element has a similar morphology and surface ornament (Extended Data Fig. 3a–d), even in an abnormal claw where element tips are flat instead of pointed (Extended Data Fig. 3h). The proximal bases of the innermost constituent elements are associated with pigmented tissue (Fig. 1e and Extended Data Fig. 3e–h).

The jaws of *E. kanangrensis* represent a modified set of trunk appendages[23] whose paired sclerites exhibit two distinct morphologies: the outer sclerite (Fig. 1j) resembles a claw, but has one or two accessory denticles on its concave edge; the inner sclerite (Fig. 1i) bears six to eight accessory denticles. These sclerites each comprise two stacked elements; the distal outline of each internal constituent element corresponds to the outline of its containing element enlarged by 2.4 ± 2.7% (Extended Data Fig. 1). Proximally, the internal element is truncated with respect to its containing element; thus all elements terminate along a common basal line (Fig. 1f and Extended Data Fig. 3g). The constituent elements of the jaw are separated by 21° of displacement along a logarithmic curve denoted by the parameters $W = 3$, $T = 0$, $D = 8$.

We regard the internal constituent elements in the claws and jaws of *E. kanangrensis* as future replacements of the outermost element. This is supported by the uniform shape and sculpture of the constituent elements within both claws and jaws, the tendency of each element to increase in size relative to its container, the separation of elements upon mechanical preparation, and the logarithmic trajectory of successive elements. The presence of a single constituent element in shed onychophoran exuviae[23,24] indicates that two to three elements characterize the intermoult individual; this suggests that ecdysis involves discarding the outermost element, secreting a new innermost element, and extending the bases of all existing elements—presumably via the pigmented basal tissue.

The constituent elements of *E. kanangrensis* jaws and claws are distinct from the superimposed sclerites found in some ecdysozoans. The duplicated sclerites that occur in certain Palaeozoic lobopodians and palaeoscolecids[7,8] represent the displacement of one individual sclerite by another during growth; upon completion of ecdysis, the displaced sclerite would have been shed. In such cases, each element is fully grown when it is sclerotized, so each internal element extends proximally beyond the margin of its containing element; this is not the case in onychophorans. Some euarthropods, such as ostracods and spinicaudatan branchiopods, retain multiple exuviae after ecdysis[25]; here, overlying moults are retained on the carapace during ontogeny, and continue to accumulate as the individual grows. This contrasts with the stacked elements in *Euperipatoides*, the outermost of which is shed during ecdysis[24]. Unlike the elements of onychophoran sclerites, the overlying exuvia of the former crustacean carapace does not correspond morphologically with the underlying exuviae; nor does it share a common

[1]Department of Earth Sciences, Downing Site, University of Cambridge, Cambridge CB2 3EQ, UK.

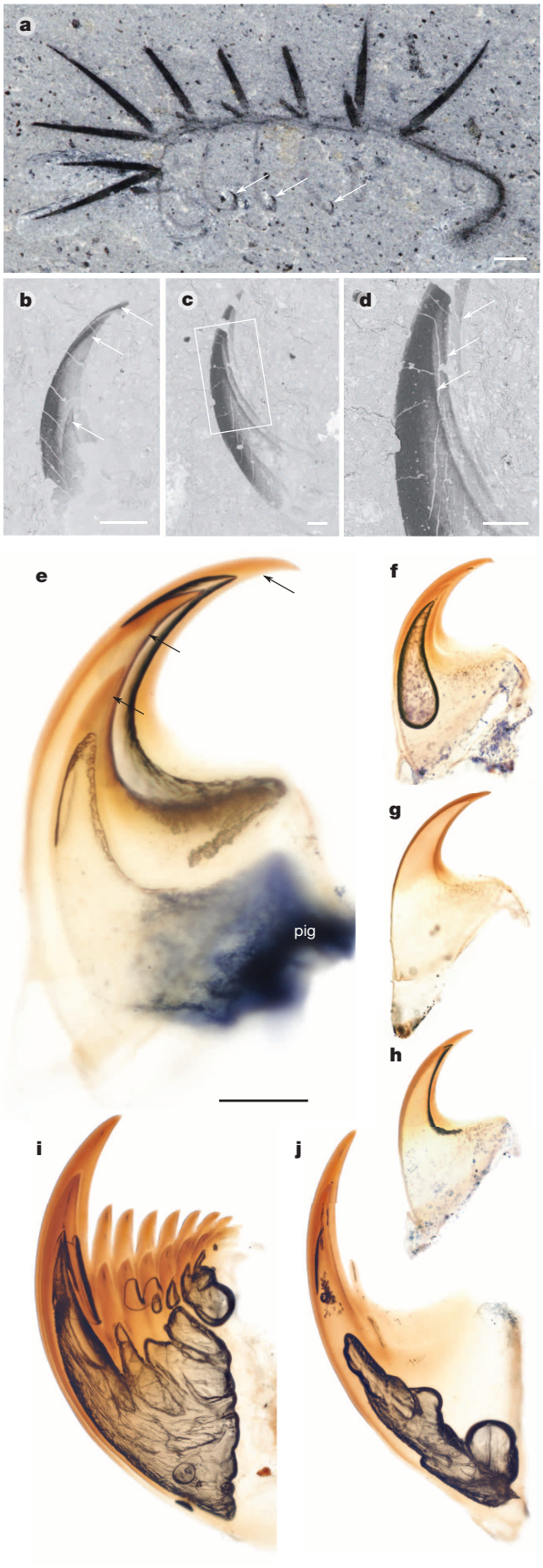

Figure 1 | Appendicular sclerites in *H. sparsa* and *E. kanangrensis*. **a**–**d**, *H. sparsa*. **a**, Royal Ontario Museum (ROM) 61124, exhibiting dorsal armature sclerites (spines) and appendicular sclerites (claws, arrowed; image courtesy of J.-B. Caron); **b**, ROM 63051, single claw with three constituent elements, innermost partly dissociated, cf. **e**; **c**, **d**, ROM 57776, claw with three intact constituent elements (image courtesy of J.-B. Caron). **e**–**j**, *E. kanangrensis* (Onychophora, Recent). **e**–**h**, Claws; **e**, air bubble between middle and outer elements; basal pigmented tissue (pig); **f**–**h**, pair of claws from single limb (**f**, single claw comprising three stacked elements; **g**, **h**, single claw separated into outer element (**g**) two stacked inner elements (**h**)); **i**, **j**, jaw sclerites, with two constituent elements (**i**, inner jaw sclerite; **j**, outer jaw sclerite). Scale bars, **a**, 1,000 μm; **b**–**d**, 100 μm; **e**, 40 μm; **f**–**j**, 100 μm.

baseline contact with the epidermal tissue. Thus the constituent elements of onychophoran claws and jaws neither represent superposition during moulting, nor the partial retention of moult exuviae; rather, they reflect the early formation of future moult elements. Being absent in Euarthropoda or Tardigrada (Extended Data Fig. 4a, b), this feature is diagnostic of Onychophora.

An onychophoran-like mode of development is inferred for the claws and spines of *H. sparsa*, which also exhibit multiple constituent elements, logarithmic growth from a basal accretionary zone, consistent morphology during growth and—verified at least on the dorsal spines—a scaly ornament on the proximal region. Taken together, these features support the homology between the claws of hallucigeniid lobopodians and the appendicular sclerites of extant onychophorans, also identifying enigmatic organic-walled microfossils as claws of stem-onychophorans (Extended Data Fig. 4c–e). This distinctive mode of growth suggests that a common process regulated the development of armature sclerites and appendicular sclerites in *H. sparsa*, despite their different locations. This could represent a shared evolutionary origin, perhaps as armour plates on an ancestral worm-like ecdysozoan[26], or the expression of limb-patterning genes in a novel location; a similar situation is observed in extant insects, where limb-patterning genes (for example, *Distal-less*) are associated with the development of ventral appendages as well as dorsal structures that may not have an appendicular origin (for example, wings)[27].

To test the homology of the stacked elements in onychophorans and *H. sparsa*, we analysed the evolutionary relationships of Palaeozoic lobopodians. Our data matrix is informed by recent findings on the segmental organization of the panarthropod head (Supplementary Note 1), and yields a substantially resolved strict consensus tree that is robust to a wide range of homology penalization—indicating a strong phylogenetic signal. The resultant topology consistently recovers *H. sparsa* and Onychophora in a clade that ancestrally bore tall spines, characterized by differentiated deutocerebral appendages and sclerites constructed from stacked constituent elements (Supplementary Note 2, transformation series 34–35, 10, 39)—indicating that the latter represents an evolutionary innovation of total-group Onychophora (Fig. 2). Palaeozoic lobopodians are recovered as paraphyletic[5,11,12,14,21], and can be broadly categorized according to their position relative to panarthropod crown groups. *Aysheaia* is the only taxon resolved in the stem-lineage of Panarthropoda (*per* refs 1, 21; *contra* refs 3, 11, 14); an alternative—but less supported—position within stem-Euarthropoda was only recovered at low concavity values (28% of those sampled; see Supplementary Data). The results indicate a major dichotomy within Panarthropoda. On one side of this basal split is total-group Onychophora, defined by the limbless posterior extension of the lobopodous trunk, undifferentiated posterior appendages and the loss of radially symmetrical circumoral structures (Supplementary Note 2, transformation series 61, 63, 19). Stem-group Onychophora includes *Diania* (*contra* refs 5, 11), *Xenusion*, *Paucipodia*, *Antennacanthopodia* and all lobopodians with sclerotized dorsal elements except *Onychodictyon ferox*[9]. *Luolishania* and the Emu Bay Shale "Collins' monster" occupy a derived position within a paraphyletic *Hallucigenia* grade. *Antennacanthopodia* and *Ilyodes* represent the closest relatives of Onychophora, indicating the secondary loss of dorsal sclerotized elements in the crown group.

On the other side of the basal panarthropod split, our analysis recovers a second major clade that includes the tardigrade and euarthropod

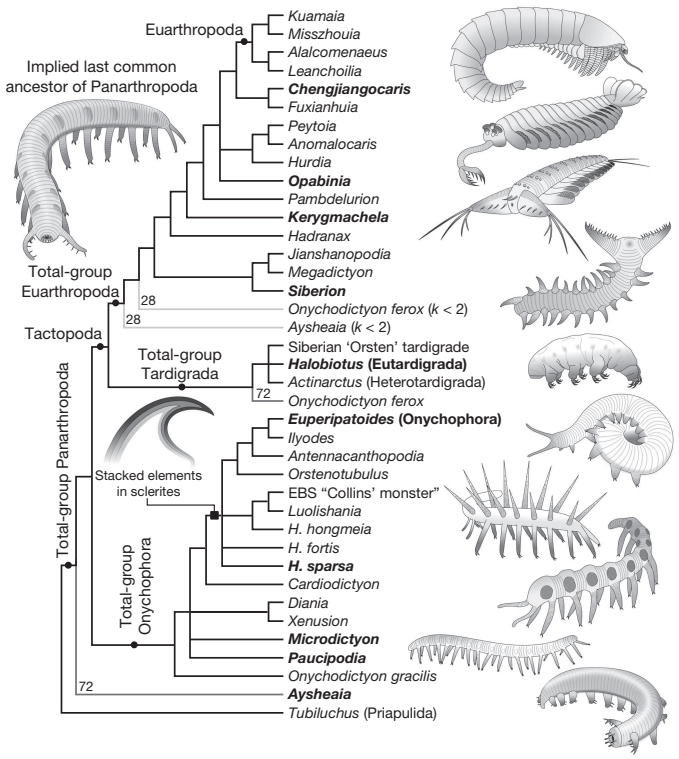

Figure 2 | Panarthropod phylogeny. Strict consensus of all most parsimonious trees recovered under equal weights (concavity constant $k = \infty$) and implied weights at 99 values of k (all most parsimonious trees listed in Supplementary Data). The origin of stacked elements in sclerites is reconstructed assuming their absence in *Cardiodictyon*; a deeper origin is possible otherwise. Nodes are annotated with the percentage of weighting parameters (values of k) that support the node (values of 100% are not shown). Illustrated taxa are marked in bold type; the morphology of the ancestral panarthropod is inferred from the most parsimonious character distribution (Supplementary Note 2). EBS, Emu Bay Shale.

total groups as sister taxa (*per* refs 10, 14, 15 and *contra* a more conventional grouping of Euarthropoda + Onychophora[28,29]), ancestrally bearing radially symmetric circumoral structures, appendicules on the lobopodous limbs and a modified posterior trunk appendage (Supplementary Note 2, transformation series 19, 49, 63). This result corroborates the Tactopoda hypothesis[10], which has recently been reinvigorated by the pattern of 'tritocerebral' innervation of the stomatogastric ganglion[17], the segmentally ganglionated nerve cord with a parasegmental organization[16] and the metamerically arranged longitudinal musculature shared between these phyla[18,19]. Within this framework, *Onychodictyon ferox*[9] is resolved as a stem-group tardigrade—consistent with hypotheses that the microscopic size of tardigrades is derived and that lobopodians include ancestors of this phylum[1,4,13,15]. An alternative position for *O. ferox* in stem-Euarthropoda was also recovered, but only at exceedingly low concavity values. Total-group Euarthropoda includes various disparate forms united by the ancestral presence of fused protocerebral appendages bearing series of spines/spinules, ultimately transformed into the euarthropod labrum[9,20] (Supplementary Note 2, transformation series 12–17). The gradual evolutionary transition from lobopodians with spinose frontal appendages (*Jianshanopodia*, *Megadictyon*) through gilled lobopodians (*Kerygmachela*, *Pambdelurion*, *Opabinia*) and anomalocaridid-type taxa (*Peytoia*, *Anomalocaris*, *Hurdia*) to stem euarthropods with full body arthrodization (for example, fuxianhuiids) is in overall agreement with previous reports[5,11,14,20]. These relationships reveal the parallel evolution of key innovations associated with the origins of panarthropod phyla; for example, the independent ventral migration of the mouth in crown-Onychophora[9], Heterotardigrada[16] and stem-Euarthropoda[20], and the non-homology between the lip papillae of Onychophora[9,30] and the circumoral structures that support Tactopoda (for example, lamellae in Tardigrada[19], radial mouthparts in anomalocaridids[21]).

The finding that sclerites with stacked constituent elements are diagnostic of total-group Onychophora, in combination with a developmentally informed phylogenetic analysis, fundamentally improves the resolution of panarthropod relationships relative to their lobopodian ancestors. Consistent with the basal position of *Aysheaia*, *Siberion* and *Onychodictyon* species within their respective stem-lineages, our analysis indicates that the ancestral panarthropod was probably a macroscopic lobopodian with heteronomous body annulations, an anterior-facing mouth with radial circumoral papillae, and paired dorsolateral epidermal specializations associated with paired lobopodous limbs that bore simple terminal claws (Supplementary Note 2, transformation series 31, 18–20, 32, 1, 5, 52, 39).

Online Content Methods, along with any additional Extended Data display items and Source Data, are available in the online version of the paper; references unique to these sections appear only in the online paper.

Received 5 March; accepted 11 June 2014.
Published online 17 August 2014.

1. Whittington, H. B. The lobopod animal *Aysheaia pedunculata* Walcott, Middle Cambrian, Burgess Shale, British Columbia. *Phil. Trans. R. Soc. Lond. B* **284,** 165–197 (1978).
2. Hou, X.-G. & Bergström, J. Cambrian lobopodians–ancestors of extant onychophorans? *Zool. J. Linn. Soc.* **114,** 3–19 (1995).
3. Ramsköld, L. & Chen, J.-Y. in *Arthropod Fossils and Phylogeny* (ed. Edgecombe, G. D.) 107–150 (Columbia Univ. Press, 1998).
4. Bergström, J. & Hou, X. Cambrian Onychophora or xenusians. *Zool. Anz.* **240,** 237–245 (2001).
5. Ma, X., Edgecombe, G. D., Legg, D. A. & Hou, X. The morphology and phylogenetic position of the Cambrian lobopodian *Diania cactiformis*. *J. Syst. Palaeontol.* **12,** 445–457 (2014).
6. Caron, J.-B., Smith, M. R. & Harvey, T. H. P. Beyond the Burgess Shale: Cambrian microfossils track the rise and fall of hallucigeniid lobopodians. *Proc. R. Soc. B* **280,** 20131613 (2013).
7. Topper, T. P., Skovsted, C. B., Peel, J. S. & Harper, D. A. T. Moulting in the lobopodian *Onychodictyon* from the lower Cambrian of Greenland. *Lethaia* **46,** 490–495 (2013).
8. Steiner, M., Hu, S.-X., Liu, J. & Keupp, H. A new species of *Hallucigenia* from the Cambrian Stage 4 Wulongqing Formation of Yunnan (South China) and the structure of sclerites in lobopodians. *Bull. Geosci.* **87,** 107–124 (2012).
9. Ou, Q., Shu, D. & Mayer, G. Cambrian lobopodians and extant onychophorans provide new insights into early cephalization in Panarthropoda. *Nature Commun.* **3,** 1261 (2012).
10. Budd, G. E. Tardigrades as 'stem-group arthropods': the evidence from the Cambrian fauna. *Zool. Anz.* **240,** 265–279 (2001).
11. Liu, J. *et al.* An armoured Cambrian lobopodian from China with arthropod-like appendages. *Nature* **470,** 526–530 (2011).
12. Legg, D. A. *et al.* Lobopodian phylogeny reanalysed. *Nature* **476,** http://dx.doi.org/10.1038/nature10267 (10 August 2011).
13. Budd, G. E. The morphology of *Opabinia regalis* and the reconstruction of the arthropod stem-group. *Lethaia* **29,** 1–14 (1996).
14. Wills, M. A., Briggs, D. E. G., Fortey, R. A., Wilkinson, M. & Sneath, P. H. A. in *Arthropod Fossils and Phylogeny* (ed. Edgecombe, G. D.) 33–105 (Columbia Univ. Press, 1998).
15. Dewel, R. A., Budd, G. E., Castano, D. F. & Dewel, W. C. The organization of the subesophageal nervous system in tardigrades: insights into the evolution of the arthropod hypostome and tritocerebrum. *Zool. Anz.* **238,** 191–203 (1999).
16. Mayer, G., Kauschke, S., Rüdiger, J. & Stevenson, P. A. Neural markers reveal a one-segmented head in tardigrades (water bears). *PLoS ONE* **8,** e59090 (2013).
17. Mayer, G. *et al.* Selective neuronal staining in tardigrades and onychophorans provides insights into the evolution of segmental ganglia in panarthropods. *BMC Evol. Biol.* **13,** 230 (2013).
18. Marchioro, T. *et al.* Somatic musculature of Tardigrada: phylogenetic signal and metameric patterns. *Zool. J. Linn. Soc.* **169,** 580–603 (2013).
19. Schulze, C. & Schmidt-Rhaesa, A. Organisation of the musculature of *Batillipes pennaki*. *Meiofauna Mar.* **19,** 195–207 (2011).
20. Budd, G. E. A palaeontological solution to the arthropod head problem. *Nature* **417,** 271–275 (2002).
21. Daley, A. C., Budd, G. E., Caron, J.-B., Edgecombe, G. D. & Collins, D. H. The Burgess Shale anomalocaridid *Hurdia* and its significance for early euarthropod evolution. *Science* **323,** 1597–1600 (2009).
22. Raup, D. M. Geometric analysis of shell coiling; general problems. *J. Paleontol.* **40,** 1178–1190 (1966).
23. De Sena Oliveira, I. & Mayer, G. Apodemes associated with limbs support serial homology of claws and jaws in Onychophora (velvet worms). *J. Morphol.* **274,** 1180–1190 (2013).

24. Robson, E. A. The cuticle of *Peripatopsis moseleyi*. *Q. J. Microsc. Sci.* **s3–105,** 281–299 (1964).
25. Olempska, E. Morphology and affinities of *Eridostracina*: Palaeozoic ostracods with moult retention. *Hydrobiologia* **688,** 139–165 (2011).
26. Dzik, J. & Krumbiegel, G. The oldest 'onychophoran' *Xenusion*: a link connecting phyla? *Lethaia* **22,** 169–181 (1989).
27. Engel, M. S., Davis, S. R. & Prokon, J. in *Arthropod Biology and Evolution* (eds Minelli, A., Boxshall, G. & Fusco, G.) 269–298 (Springer, 2013).
28. Rota-Stabelli, O. *et al.* A congruent solution to arthropod phylogeny: phylogenomics, microRNAs and morphology support monophyletic Mandibulata. *Proc. R. Soc. B* **278,** 298–306 (2011).
29. Campbell, L. I. *et al.* MicroRNAs and phylogenomics resolve the relationships of Tardigrada and suggest that velvet worms are the sister group of Arthropoda. *Proc. Natl Acad. Sci. USA* **108,** 15920–15924 (2011).
30. Martin, C. & Mayer, G. Neuronal tracing of oral nerves in a velvet worm—implications for the evolution of the ecdysozoan brain. *Front. Neuroanat.* **8,** 7 (2014).

Supplementary Information is available in the online version of the paper.

Acknowledgements The authors are supported by Research Fellowships at Clare College (M.R.S.) and Emmanuel College (J.O.-H.), University of Cambridge, UK. Thanks to J.-B. Caron and T. Harvey for images, access to material and discussions. D. Erwin, K. Hollis and P. Fenton facilitated access to museum specimens, and S. Whittaker assisted with electron microscopy. *E. kanangrensis* were collected from the Blue Mountains, New South Wales, with assistance from G. Budd and N. Tait and funding from an H.B. Whittington Research Grant (Paleontological Society). N. Butterfield and R. Janssen provided additional material. Parks Canada provided research and collection permits to Royal Ontario Museum teams led by D. Collins. The software TNT is funded by the Willi Hennig Society.

Author Contributions M.R.S. conceived the project; dissected, described and interpreted specimens; and ran the phylogenetic analysis. J.O.-H. led the integration of developmental data into phylogenetic analysis and the interpretation of results. Both authors contributed equally to data analysis, discussion of results and manuscript preparation.

Author Information Reprints and permissions information is available at www.nature.com/reprints. The authors declare no competing financial interests. Readers are welcome to comment on the online version of the paper. Correspondence and requests for materials should be addressed to M.R.S. (ms609@cam.ac.uk).

METHODS

Weighting strategies. Under equal weights, each additional step in a tree topology is penalized equally. Taking an example from Goloboff[31], if transformation series *A* has one step on tree *X* and two steps on tree *Y*, whereas transformation series *B* has 15 steps on tree *X* and 14 steps on tree *Y*, trees *X* and *Y* each contain 16 steps in total and are thus treated as equally plausible. Implied weighting assumes that an additional step in a highly homoplastic transformation series is preferable to an additional step in a less homoplastic transformation series: that is, it is more parsimonious to add a 15th step to transformation series *B*, which is already highly homoplasious, than it is to add a second step to transformation series *A*, which otherwise exhibits no homoplasy.

Successive weighting[32] represents an iterative solution to this problem, calculating the homoplasy of each transformation series under an equally weighted tree, then repeating the analysis using characters' consistency index to repeat the analysis. This approach suffers from circularity; it generates different results from different starting points. The method of Goloboff[31] circumvents this problem by penalizing each additional step in a transformation series less strongly than the step before, thus weighting each transformation series according to its consistency with each evaluated tree. The penalty attached to subsequent steps decreases at a rate set by a concavity constant, *k*; the lower the concavity constant, the less weight is attached to subsequent steps.

With a small concavity constant, transformation series that have one or more additional steps are down-weighted to the point of irrelevance. At $k < 1.5$, a tree *X* where transformation series *A* has no additional steps and transformation series *B* has six additional steps will be preferred to a tree *Y* where both transformation series have a single additional step. At $k < 1$, transformation series *B* can have any number of steps on tree *X*, and tree *X* will still be preferred to tree *Y*. Thus $k < 1$ corresponds to a stance that transformation series either represent homologies or contain no phylogenetic information at all: if a transformation has occurred more than once, it is (almost) no more likely to appear twice than it is to appear 100 times. This approach is overly aggressive; indeed, $k < 2$ is rarely seen in the literature.

With a larger concavity constant ($k > 30$, perhaps), characters with additional steps are scarcely down-weighted; implied weighting under large values of *k* approximates equal weighting. An intermediate value is therefore most suitable, but there is no objective means to select this value. Values of *k* between 3 and 5 are typical, although the most appropriate value varies with the number of terminals (and thus opportunity for homoplasy) in a data set[31]. One way to approach this issue is to repeat an analysis over a range of values of *k*, and to identify the strict consensus of these possible trees[33]. Rather than select a narrow range of values, we took 99 values of *k* from a log-normal distribution, with mean = 5 and s.d. = 5, so as to exhaustively sample parameter space. The strict consensus of most parsimonious trees for each value of *k*, generated using the parsimony ratchet[34] and sectorial search[35] heuristics in TNT[36,37], is reported in the Supplementary Data. Figure 2 displays the consensus of all most parsimonious trees recovered at all sampled values of *k* (0.12–210) and the equal weights tree.

Removal of transformation series. If transformation series 39 ('sclerites consist of a stack of constituent elements') is excluded from the analysis, an identical topology is recovered for all values of *k*, demonstrating that homology between the stacked elements of onychophoran claws and the claws of *Hallucigenia sparsa* is supported even if the character is not reflected in the input matrix.

31. Goloboff, P. A. Estimating character weights during tree search. *Cladistics* **9,** 83–91 (1993).
32. Farris, J. S. A successive approximations approach to character weighting. *Syst. Biol.* **18,** 374–385 (1969).
33. Mirande, J. M. Weighted parsimony phylogeny of the family Characidae (Teleostei: Characiformes). *Cladistics* **25,** 574–613 (2009).
34. Nixon, K. C. The Parsimony Ratchet, a new method for rapid parsimony analysis. *Cladistics* **15,** 407–414 (1999).
35. Goloboff, P. A. Analyzing large data sets in reasonable times: solutions for composite optima. *Cladistics* **15,** 415–428 (1999).
36. Goloboff, P. A., Farris, J. & Nixon, K. TNT: tree analysis using new technology. (http://www.lillo.org.ar/phylogeny/tnt/, 2003).
37. Goloboff, P. A., Farris, J. S. & Nixon, K. C. TNT, a free program for phylogenetic analysis. *Cladistics* **24,** 774–786 (2008).
38. Campiglia, S. & Lavallard, R. in *Proc. 7th Int. Congr. Myriapodology* (ed. Minelli, A.) 461 (E. J. Brill, 1990).
39. Harvey, T. H. P., Ortega-Hernández, J., Lin, J.-P., Zhao, Y. & Butterfield, N. J. Burgess Shale-type microfossils from the middle Cambrian Kaili Formation, Guizhou Province, China. *Acta Palaeontol. Pol.* **57,** 423–436 (2012).

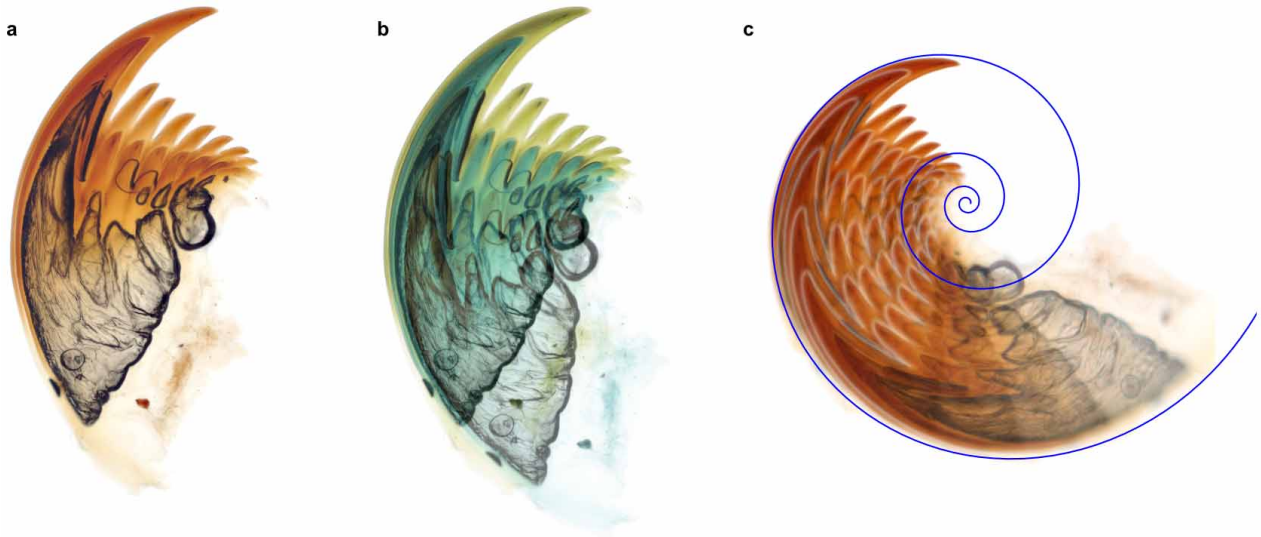

Extended Data Figure 1 | Claw measurements. To reconstruct the relationship between the stacked constituent elements, a digital image of a sclerite (**a**) was duplicated, rotated and enlarged such that its outer sclerite precisely overlay the inner sclerite in the original image (**b**; the cyan image has been enlarged by 5% and rotated to match the inner sclerite in the yellow image). Repetition of this process demonstrates a logarithmic growth trajectory (**c**); a logarithmic spiral was fitted to this trajectory and its Raupian parameters[22] calculated. This process was most accurate in the inner jaw elements, whose dentate margin provided multiple landmarks that allowed the precise fitting of subsequent images. Estimates were also obtained for the outer jaws and appendicular claws of *Euperipatoides*, and the claws and spines of *H. sparsa*. *Hallucigenia* spines demonstrated variability in Raup's *D* because they are sometimes obliquely preserved, so the maximum value was taken as representative. The implied growth rate of 2.4 ± 2.7% in *Euperipatoides* sclerites (range 0–8%; measured from five inner and six outer jaw sclerites) cannot persist throughout the organism's lifespan, since moulting consistently occurs every 2 weeks (ref. 38). Either moulting occurs less frequently in wild populations, the rate of growth varies during ontogeny or the constituent elements deform slightly during growth.

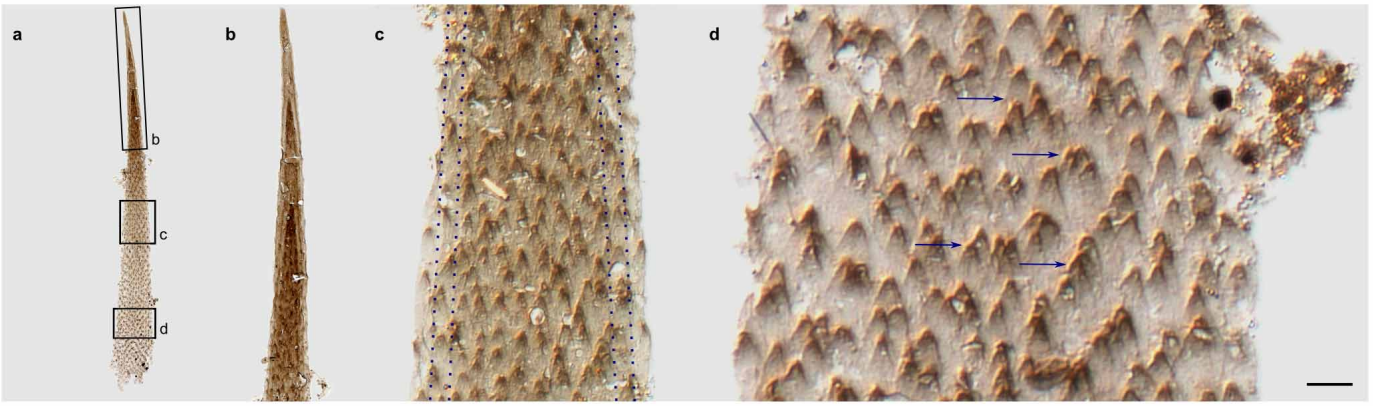

Extended Data Figure 2 | Density of scaly ornament in a hallucigeniid spine with three constituent elements (Geological Survey of Canada 136958). **a**, Complete spine, showing regions of enlargement; **b**, apex of spine showing tips of two internal elements; **c**, margins of two internal elements faintly visible (dotted lines); density of scales where three elements are superimposed is 0.050 scales per square micrometre; where two elements are superimposed it is 0.039 scales per square micrometre; for a single element it is 0.026 scales per square micrometre; slight deviation from a 3:2:1 ratio is attributed to decreased visibility of individual scales in occluded regions; **d**, up to five scales overlap; only two could overlap if scales were restricted to the front and back surfaces of a single element. Transmitted light images from multiple focal planes combined using CombineZM (A. Hadley). Scale bar, **a**, 100 μm; **b**, 40 μm; **c**, 10 μm; **d**, 5 μm.

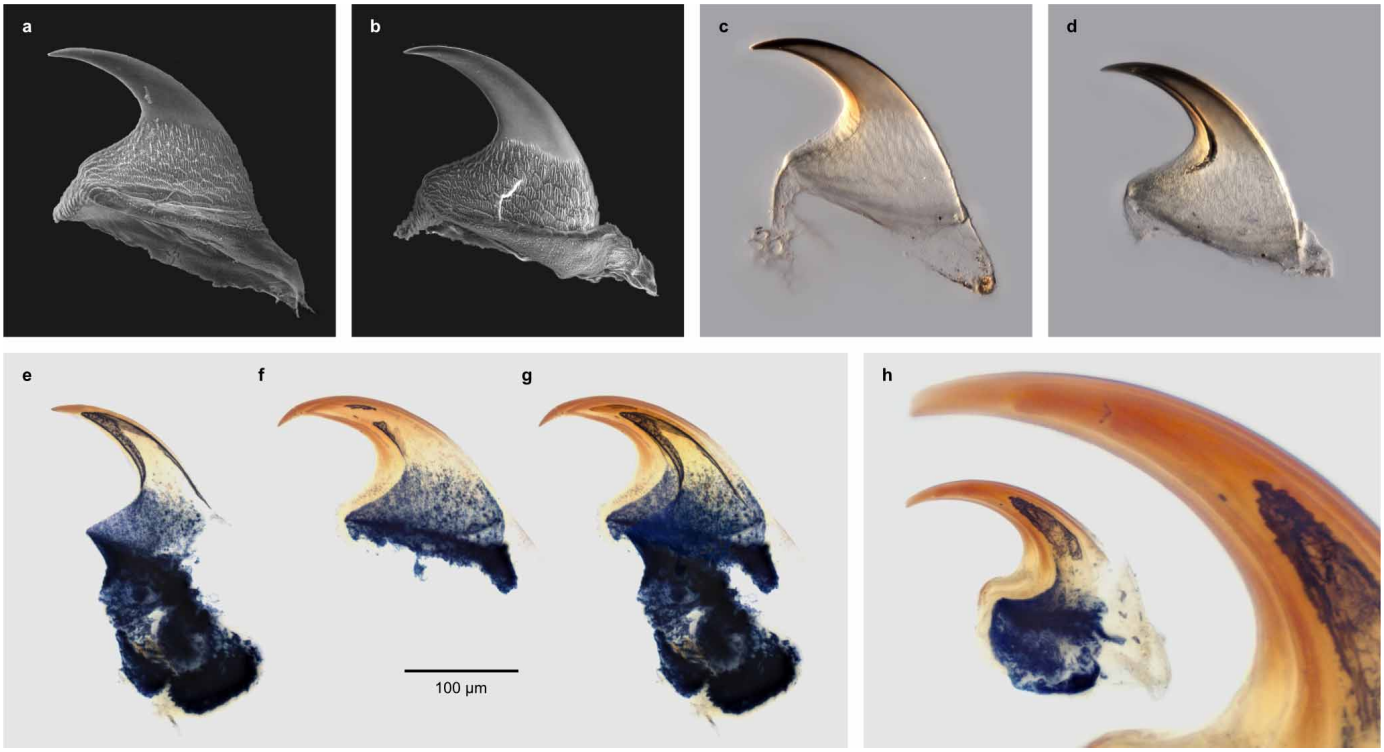

Extended Data Figure 3 | Claws of *Euperipatoides kanangrensis* (Onychophora). **a**, **b**, Secondary electron images of a single claw, separated into outermost element (**a**) and inner elements (**b**), each with ornamented basal region. **c**, **d**, Differential image contrast images of a single claw, separated into outermost element (**c**) and inner elements (**d**). Nomarski interference contrast accentuates the basal ornament. **e–g**, Single claw, separated into innermost element (**e**) and outer elements (**f**); pigmented foot tissue only associated with inner two elements; **g**, digital superposition of **e** and **f** showing original claw construction. **h**, Abnormal claw with blunt tip reflected in each constituent element. Transmitted light images from multiple focal planes combined using TuFuse (M. Lyons). Scale bar, 100 µm.

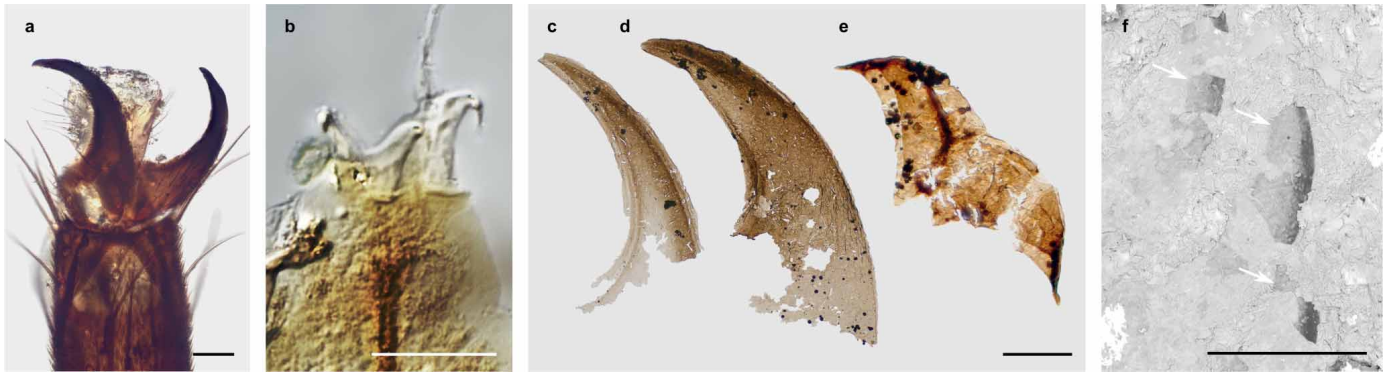

Extended Data Figure 4 | Sclerite constitution in other taxa. **a**, **b**, Single constituent element in claws of (**a**) *Nephrotoma* spp. (Tipulidae, Hexapoda, Euarthropoda) and (**b**) Eutardigrada (species indeterminate). Nomarski interference contrast. **c–e**, Small carbonaceous fossils with stacked constituent elements, interpreted as appendicular sclerites of total-group onychophorans (images courtesy of T. Harvey): **c**, **d**, from the basal mid-Cambrian (Stage 5) Kaili biota[39]; **e**, articulated pair from the mid- to late Cambrian Deadwood Formation, each claw comprising two constituent elements. **f**, Three appendicular sclerites (claws: arrowed) from a single appendage of *Aysheaia pedunculata* from the mid-Cambrian Burgess Shale (ROM 63052), each comprising a single element. Transmitted light images from multiple focal planes combined using TuFuse (M. Lyons) and CombineZM (A. Hadley). Scale bars, 100 μm.